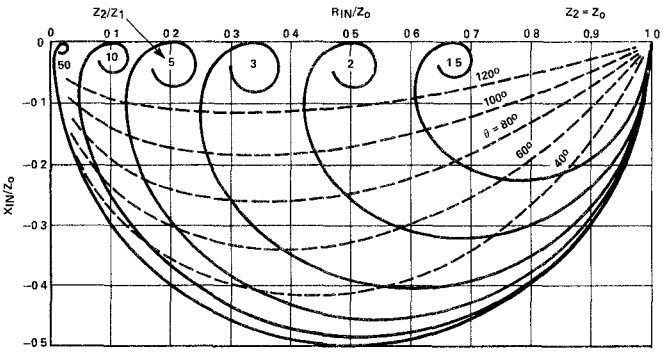

Fig. 2. Normalized input impedance of the exponentially tapered transmission line for various impedance transformation ratios (Z_2/Z_1) and electrical length (θ). The high impedance end of the taper matches the system impedance ($Z_2 = Z_1$).

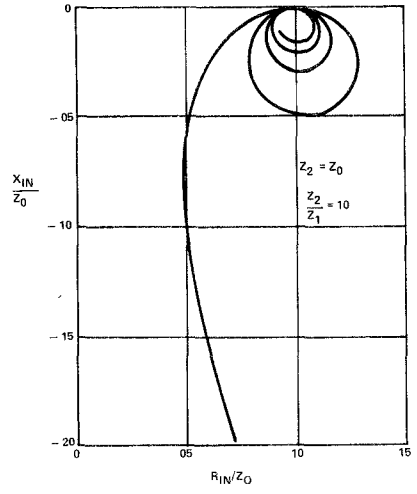

Fig. 3. Enlarged view of a portion of Fig. 2 showing the behavior of the normalized input impedance for tapers up to several wavelengths long. The impedance transformation ratio $Z_2/Z_1 = 10$.

At an electrical length of approximately 200° the input impedance becomes real. For longer electrical lengths the impedance follows a small spiral, becoming real again at one wavelength. Further increase in length causes the impedance to follow a smaller spiral, and each additional half-wavelength introduces another even smaller spiral, the impedance becoming real at each multiple of a half-wavelength.

If it is realized that, for a given physical length of line, the electrical length is proportional to the frequency, the broad-band properties of the exponential line become clear. The input impedance remains essentially constant above the frequency at which the taper length is appreciably over one-half wavelength. It should be pointed out that this broad-band characteristic applies to the transformation of real loads only. However, the behavior of the input impedance as a function of frequency may be readily determined for any other load by applying (8)–(13).

The less-well-known narrow-band properties of the exponentially tapered line are also shown in Fig. 2. For example, a transistor whose input impedance is known to be $10 + j15\ \Omega$ requires a conjugate matching impedance, normalized to $50\ \Omega$ of $0.2 - j0.3$. Finding this point on Fig. 2 reveals that this impedance is presented by an exponentially tapered line with an impedance transformation ratio of 5:1 and an electrical length of 60°. In this case, the electrical length is considerably shorter than a quarter-wavelength. Hence, the exponentially tapered line is also an attractive vehicle for narrow-band applications that require capacitive impedance transformations where small physical size is important.

CONCLUSIONS

Correction and modification of the existing closed form solution for the reflection coefficient along an exponentially tapered line has permitted the computation of curves for the input impedance which are normalized with respect to frequency and Z_0. The findings clearly demonstrate both the broad-band and narrow-band properties of the tapered line. Use of the normalized graphs will aid in the design of exponentially tapered transmission lines for practical applications.

REFERENCES

[1] C. Burrows, "The exponential transmission line," *Bell Syst. Tech. J.*, pp. 555–573, Oct. 1938.
[2] H. A. Wheeler, "Transmission lines with exponential taper," *Proc. IRE*, vol. 27, pp. 65–71, Jan. 1939.
[3] L. Walker and N. Wax, "Non-uniform transmission lines and reflection coefficients," *J. Appl. Phys.*, pp. 1043–1045, Dec. 1946.
[4] R. E. Collin, "The optimum tapered transmission line matching section," *Proc. IRE*, vol. 44, pp.539–548, Apr. 1956.
[5] R. N. Ghose, "Exponential transmission lines as resonators and transformers," *IRE Trans. Microwave Theory Tech.*, vol. MTT-5. pp. 213–217, July 1957.
[6] C. P. Womack, "The use of exponential lines in microwave components," *IRE Trans. Microwave Theory Tech.*, vol. MTT-10, pp. 124–132, Mar. 1962.
[7] V. Ramachandran, "Design charts of an exponential transmission line for impedance matching," *IEEE Trans. Circuit Theory* (Corresp.), vol. CT-10, pp. 516–520, Dec. 1963.
[8] C. Kamnitis, "Broadband matching of UHF microstrip amplifiers," *Microwaves*, pp. 54–56, Apr. 1969.

Transmission Characteristics of Spherical TE and TM Modes in Conical Waveguides

M. S. NARASIMHAN, MEMBER, IEEE, AND K. S. BALASUBRAMANYA, MEMBER, IEEE

***Abstract*—The transmission properties of spherical TE and TM modes in a perfectly conducting conical waveguide are treated in detail. To start with, an analytically simple and highly accurate digital-computer based iterative algorithm has been employed to evaluate the eigenvalues associated with the spherical TE and TM modes within the guide irrespective of the flare angle ($2\alpha_0$) of the conical waveguide ($\theta < 2\alpha_0 < 360°$). Subsequently, explicit expressions for the attenuation constant, phase constant, phase velocity, and wave impedance are obtained for the spherical modes transmitted within the guide. Accurate eigenvalues obtained numerically are used to study the variation of attenuation constant, phase constant, phase velocity, and wave impedance as a function of the radial distance from the apex with α_0 as a parameter. Measured data on the phase constant of a conical waveguide for the TE_{11} mode have been compared with the analytical results obtained by calculation and an excellent agreement between the two justifies the validity of the analysis presented. Finally, a study of the phase coherence between the dominant spherical TE and TM modes within the guide is presented which may be fruitfully employed in the design of dual-mode conical waveguides.**

I. INTRODUCTION

In several microwave systems encountered in such application as earth stations for satellite communications, microwave radio-relay links, millimeter-wave communications, and in the launching of Gaussian modes in beam waveguides [1], conical tapers and conical waveguides are frequently employed. Conical waveguides and tapers encountered in the systems just mentioned generate higher order modes, however small their amplitudes may be. Further, there has been considerable interest in the recent past in techniques which require controlled excitation of higher order modes combined with the dominant mode, as for example dual or multimoding in conical waveguides. One application of such a multimode waveguide will be in low-noise antennas for satellite communications [2].

All applications of conical waveguides mentioned previously involve generation and transmission of spherical TE and TM modes of different orders. Further, a common feature of dual or multi-

Manuscript received March 28, 1974; revised July 18, 1974.
The authors are with the Department of Electrical Engineering, Indian Institute of Technology, Madras, India.

moding techniques in a conical waveguide is the necessity for maintaining a high degree of phase coherence among the various modes. In order to design such systems and predict how frequency, temperature, and structural changes influence transmission characteristics it is necessary to study, in detail, variation of phase constant, attenuation constant, and wave impedance for different modes with radial distance in the conical waveguide.

In this short paper, to begin with, a novel method is devised for accurate evaluation of the eigenvalues associated with the propagating TE and TM modes in a conical waveguide which are subsequently used to study the transmission properties of the guide. Finally, a study of phase coherence between the TE_{11} and TM_{11} modes in a dual-mode conical waveguide has also been presented.

II. EIGENVALUES OF SPHERICAL TE AND TM MODES WITHIN THE GUIDE

The electromagnetic field components (of interest in the study of transmission characteristics) in a perfectly conducting waveguide of infinite extent are well known [3]. The eigenvalues associated with the field components are given by the nth nonvanishing root of the characteristics equations:

$$d/d\theta - [P_s^m(\cos\theta)]_{\theta=\alpha_0} = 0, \quad \text{for } TE_{m,n} \text{ modes} \tag{1}$$

$$[P_s^m(\cos\theta)]_{\theta=\alpha_0} = 0, \quad \text{for } TM_{m,n} \text{ modes.} \tag{2}$$

As mentioned previously, a systematic and detailed study of the transmission properties of spherical modes in conical waveguides requires the exact evaluation of the eigenvalues associated with the type of mode under consideration. An analytically simple and highly accurate digital-computer based iterative algorithm is described here for evaluating the exact eigenvalues. The technique described involves closed-form evaluation of the eigenvalues, based on an accurate asymptotic solution for spherical wave functions associated with modes in a conical waveguide. The eigenvalues obtained from the asymptotic solution are close to the exact values for all flare angles $1 < \alpha_0 < 180°$. Hence the asymptotic solution is used to generate the starting values for numerical evaluation of the more exact eigenvalues with simple iterative process.

An analytically simple and sufficiently accurate asymptotic solution for the required eigenvalues is obtained by considering the differential equation governing the $H(\theta)$ part of the solution for the scalar potential $u^{e,m}$ given as follows [3]:

$$\frac{1}{H\sin\theta}\frac{d}{d\theta}\left[\sin\theta\frac{dH}{d\theta}\right] + s(s+1) - \frac{m^2}{\sin^2\theta} = 0 \tag{3}$$

where, for $|\cos\theta| < 1$,

$$H = AP_s^m(\cos\theta) + BQ_s^m(\cos\theta). \tag{3a}$$

The asymptotic solution $F(\theta)$ corresponding to $H(\theta)$ is obtained by replacing $\sin\theta$ by θ in (3) and solving the resulting differential equation as detailed in [4]:

$$F(\theta) = C[J_m(q\theta) + DN_m(q\theta)] \tag{4}$$

where

$$q = [s(s+1)]^{1/2}$$

and

$$s = -0.5 + [0.25 + (p_{mn}\alpha_0)^2]^{1/2}. \tag{5}$$

In (5) "p_{mn}" and "D" depend on the type of radial waveguides considered. For example, in a conical waveguide, $D = 0$ and p_{mn} represents the nth nonvanishing root of $J_m'(x) = 0$, when TE to r modes are considered. Similarly, for TM to r modes, "p_{mn}" stands for the nth nonvanishing root of $J_m(x) = 0$. Since the roots of the Bessel functions of the first kind (integral order) and its derivative are readily available [5], "s" can be directly computed from (5). The eigenvalues obtained using (5) for an arbitrary flare $1 < \alpha_0 < 180°$ (for the TE_{1n} or TM_{1n} modes) are found to be close to the exact eigenvalue. In order to obtain the exact eigenvalues an iterative procedure is developed by considering the integral representation for the associated Legendre functions [6]:

$$P_s^m(\cos\theta) = (-1)^m\frac{(\sin\theta)^{-m}}{(m+0.5)}\left(\frac{2}{\pi}\right)^{1/2} I_1(s,\theta) \tag{6}$$

where

$$I_1(s,\theta) = \frac{(s+m+1)}{(s-m+1)}\int_0^\theta (\cos x - \cos\theta)^{m-0.5}\cos[x(s+0.5)]\,dx. \tag{7}$$

For the TE_{1n} and TM_{1n} modes the eigenvalue equations (1) and (2) may be reduced to the following forms[1] with the aid of (6):

$$G_1(s,\alpha_0) = sI(s+1,\alpha_0) - (s+1)\cos\alpha_0 I(s,\alpha_0) = 0 \tag{8a}$$

$$G_2(s,\alpha_0) = I(s,\alpha_0) = 0 \tag{8b}$$

where

$$I(s,\alpha_0) = s(s+1)\int_0^{\alpha_0} (\cos x - \cos\alpha_0)^{1/2}\cos[x(s+0.5)]\,dx$$

$$s^{(k+1)} = s^{(k)} - \frac{G_i(s^{(k)},\alpha_0)}{G_i'(s^{(k)},\alpha_0)} \tag{9}$$

where $i = 1,2$ for TE_{1n} and TM_{1m} modes, respectively,

$$G_1'(s,\alpha_0) = sI'(s+1,\alpha_0) - (s+1)\cos\alpha_0 I'(s,\alpha_0) + I(s+1,\alpha_0) - \cos\alpha_0 I(s,\alpha_0) \tag{10a}$$

$$G_2'(s,\alpha_0) = I'(s,\alpha_0) \tag{10b}$$

and

$$I'(s,\alpha_0) = (2-s+1)\int_0^{\alpha_0} (\cos x - \cos\alpha_0)^{1/2}\cos[x(s+0.5)]\,dx - s(s+1)\int_0^{\alpha_0} x(\cos x - \cos\alpha_0)^{1/2}\sin[x(s+0.5)]\,dx.$$

In (9), $s^{(k+1)}$ represents the $(k+1)$th value of "s" evaluated after k successive iterations and the known asymptotic solution for "s" given by (5) is taken as the starting value "s."

IBM 370/155 computer system was made use of for performing the successive iterations. The integrals $I(s,\alpha_0)$ and $I'(s,\alpha_0)$ were evaluated numerically using a 24 point Gaussian quadrature formula in a subprogram forming a part of the computer program meant for evaluating "s." Double-precision arithmetic was used throughout in order to obtain an accuracy of 10^{-6} while computing "s." The truncation error involved in the evaluation of the integrals $I(s,\alpha_0)$ and $I'(s,\alpha_0)$ are of the same order and is hence eliminated completely as they appear as a ratio in evaluating the eigenvalue (9). Further, since the starting values "s" (given by (5) are close to the exact eigenvalues (Fig. 1) the convergence of "s" to the required exact value has been found to be very fast. More accurate eigenvalues plotted in Fig. 1 were obtained (numerically) with less than five iterations in each case.

III. TRANSMISSION PROPERTIES OF THE TE AND TM MODES WITHIN THE GUIDE

The transmission properties of the guide are governed by a number of physical quantites. The important parameters are the attenuation and phase constants (α,β) which are defined as the logarithmic rate of decrease of amplitude and phase, respectively, of a field component in the direction of propagation. More interesting, however, is the electric field component (which is a more directly measurable physical unity) and since both E_θ and E_ϕ have the same functional dependence on "r," one may define "α" and "β" as follows:

$$\alpha + j\beta = F(x,y) = -\frac{1}{E}\frac{\partial E}{\partial r} \tag{11}$$

where E denotes either E_θ or E_ϕ for TE or TM modes.

For TE and TM modes [3], one obtains

$$F^{TE}(x,y) = k(H_y'/H_y - 1/2x) \tag{12}$$

and

[1] The recurrence relation

$$\sin\theta(dP_s^1/d\theta) = sP_{s+1}^1(\cos\theta) - (s+1)\cos\theta P_s^1(\cos\theta)$$

has been made use of for obtaining (8a) from (6).

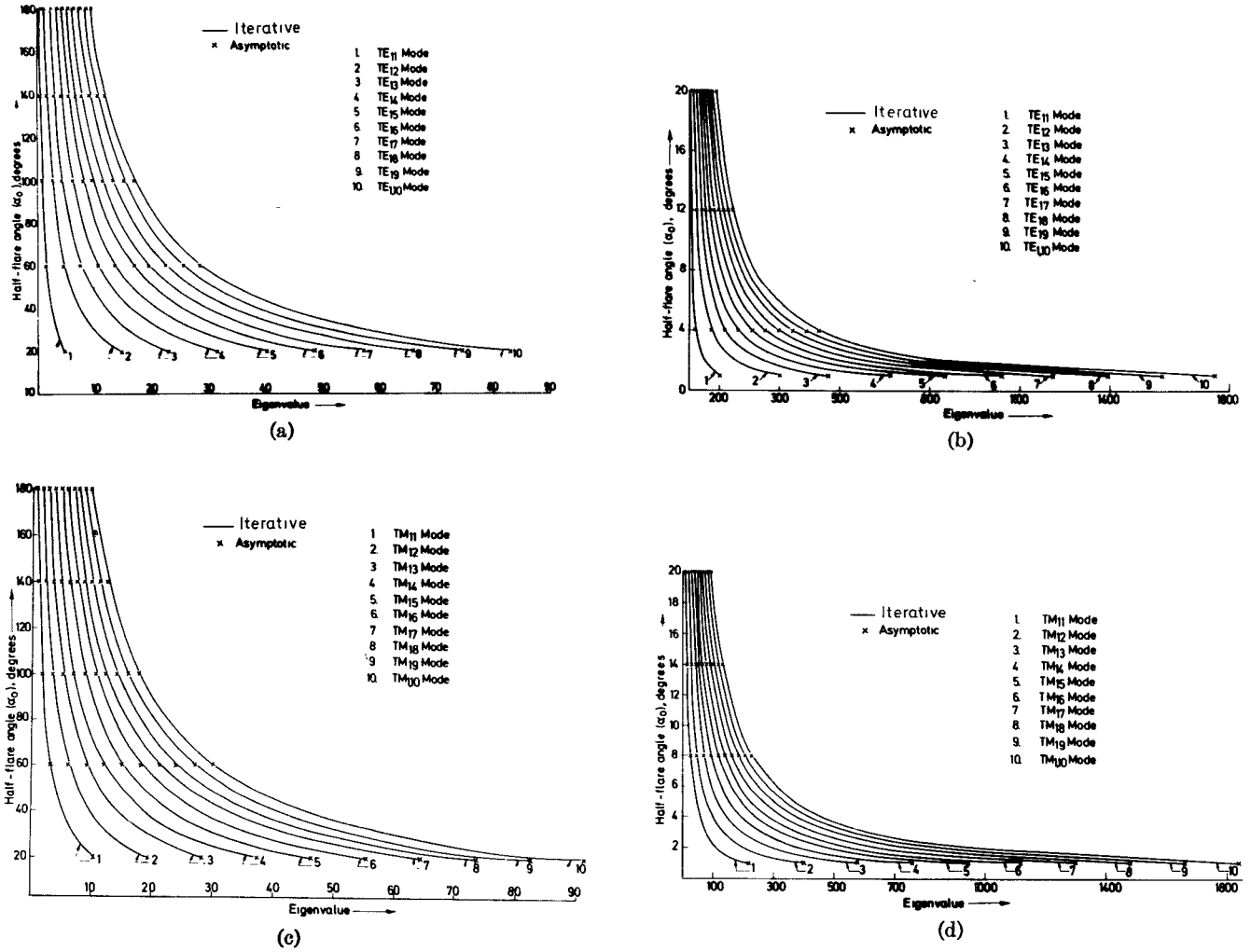

Fig. 1. Variation of eigenvalue for the TE and TM modes with α_0.

$$F^{TM}(x,y) = -k\left(\frac{H_y'' - 3H_y/4x^2}{H_y/2x + H_y'}\right) \tag{13}$$

where $H_y = H_y^{(2)}(x)$ is the Hankel function of the second kind, order y.

H_y' and H_y'' are the first and the second derivatives of the Hankel function, with respect to the argument $y = s + 0.5$ and $x = kr$. The Hankel function $H_y^{(2)}(x)$ and its derivative can be expressed as complex quantities [5] and the real and imaginary parts of $F^{TE}(x,y)$ and $F^{TM}(x,y)$ give the attenuation and phase constants, respectively, for the TE to r and TM to r modes.

The phase velocity is defined by

$$v_p = \frac{\omega}{\beta} = \frac{c}{(\beta/k)}. \tag{14}$$

Calculation of v_p requires a knowledge of the normalized phase constant (β/k) for an arbitrary flare angle $1° < \alpha_0 < 180°$.

Another parameter of particular interest associated with the mode transmission is the wave impedance, defined by

$$Z = E_\theta/H_\phi. \tag{15}$$

From [3] and (15) one obtains

$$Z^{TE} = \frac{-jZ_0[x^{1/2}H_y^{(2)}(x)]}{d/dx[x^{1/2}H_y^{(2)}(x)]} \tag{16}$$

$$Z^{TM} = \frac{jZ_0 d/dx[x^{1/2}H_y^{(2)}(x)]}{x^{1/2}H_y^{(2)}(x)}. \tag{17}$$

Based on (14), (16), and (17), a variation of α, β, v_p, and Z as a function of kr with α_0 as a parameter has been studied and the results are presented in Figs. 2–5.[2] The study reveals that close to the apex the (reactive) attenuation associated with the mode transmission is large. As "kr" increases, "β" increases and $\beta \to k$ for $kr \gg 1$. Hence one may define somewhat arbitrarily an attenuation region where $\beta \ll 1$ and a transmission where $\beta \simeq k$. However, no cutoff radius can be clearly defined. Examination of Fig. 4 reveals that in the attenuation region the phase angle between E_θ and H_ϕ is not equal to 90° as in a cylindrical guide and the phase relationship is somewhat involved.

In some applications such as the dual-mode conical waveguide horns it is necessary that the phase slip between the spherical TE_{11} and TM_{11} modes be known in order to obtain the required phase relationship between the two modes at various radial distances within the guide. When a TE to r or TM to r mode is transmitted over a distance "d" along a conical waveguide, the total phase shift over "d" is defined by

$$\Delta = \int_{\alpha_1}^{\alpha_2} \beta(x)\, dx. \tag{18}$$

In order to obtain the phase shift for the TE_{11} and TM_{11} modes as a function of "d" within the conical waveguide, the integral appearing in (18) was evaluated numerically and the results are presented in Fig. 6. The phase slip ($\Delta_1 = \Delta^{TE11} - \Delta^{TM11}$) between the two modes

[2] Explicit expressions for α^{TE}, β^{TE}, α^{TM}, and β^{TM} obtained from (12) and (13) have been used to calculate and plot the results presented in Figs. 2–5.

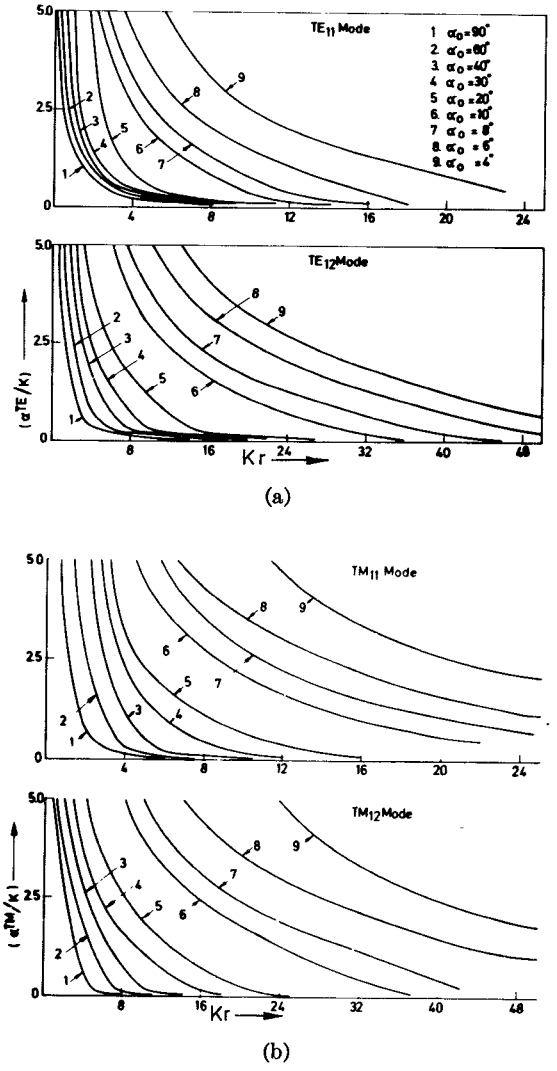

Fig. 2. Variation of the attenuation constant (α) with kr for the TE and TM modes.

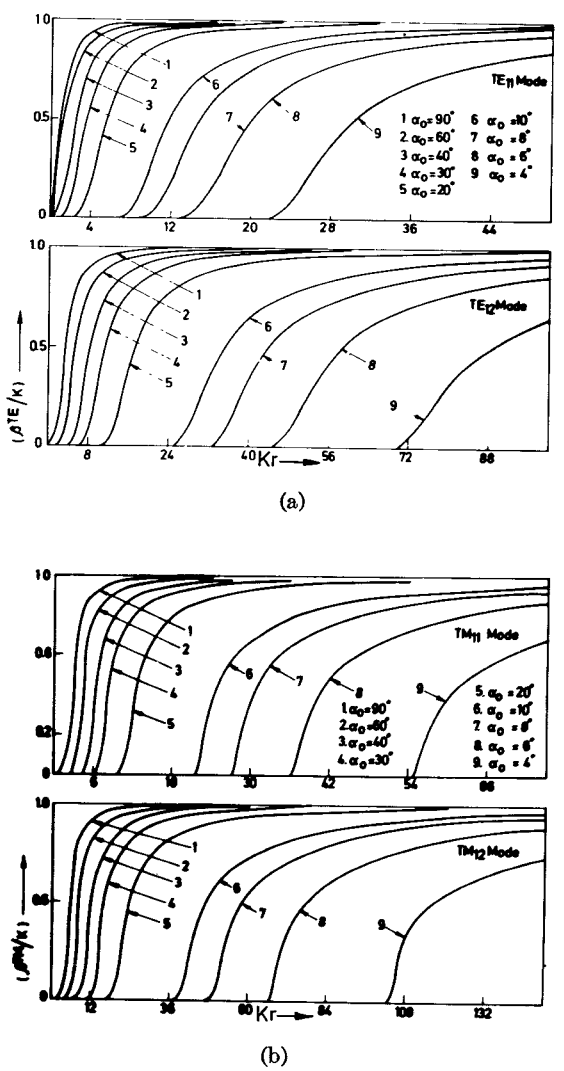

Fig. 3. Variation of the phase constant (β) with kr for the TE and TM modes.

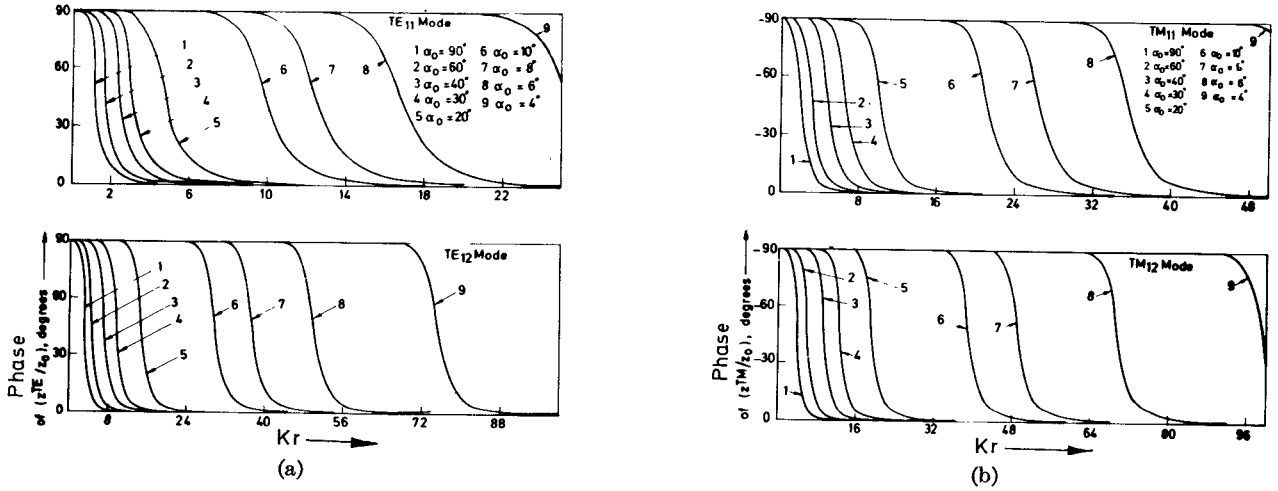

Fig. 4. Variation of the phase angle of Z (wave impedance) with kr for the TE and TM modes.

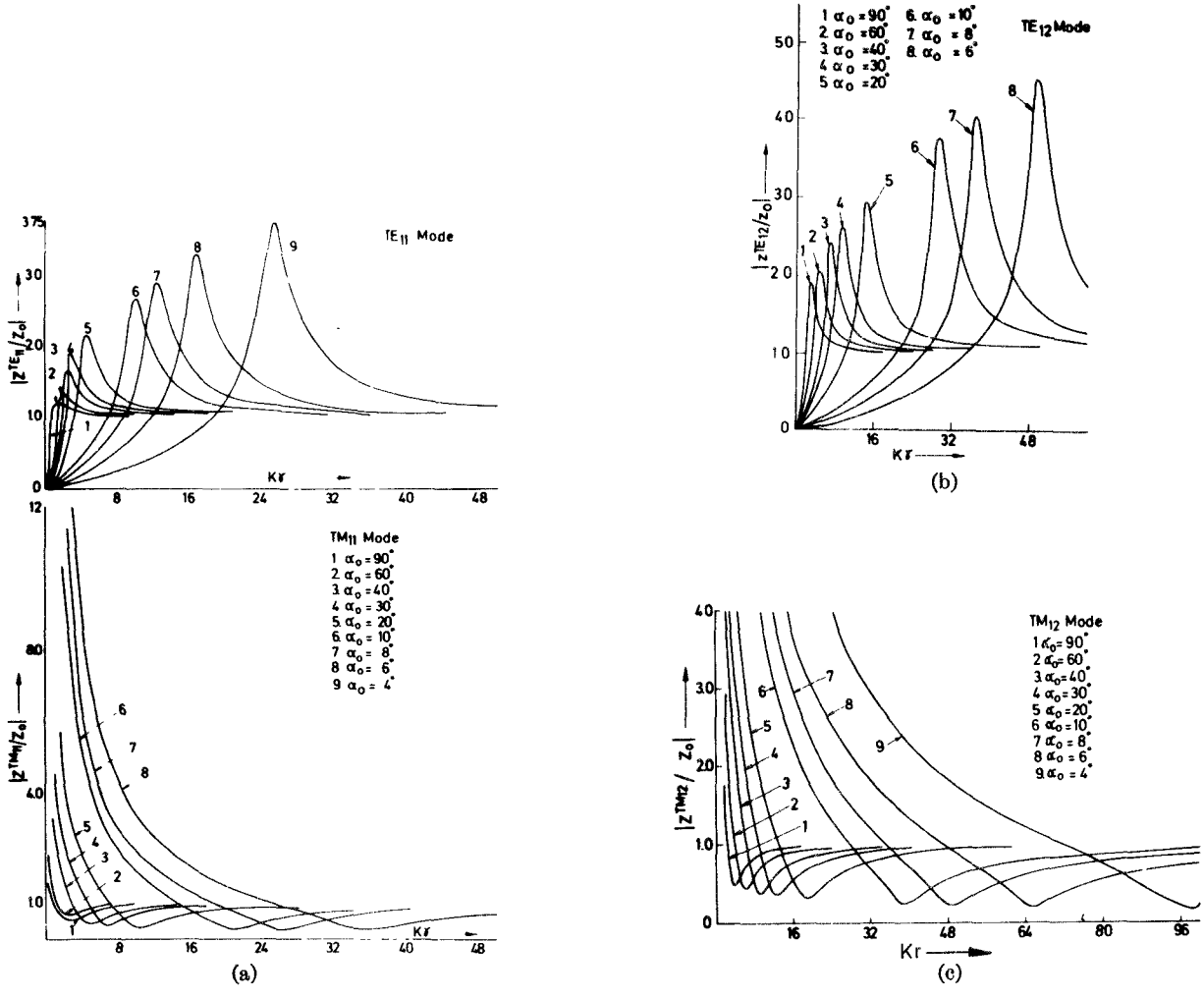

Fig. 5. Variation of $|Z|$ with kr for the TE and TM modes.

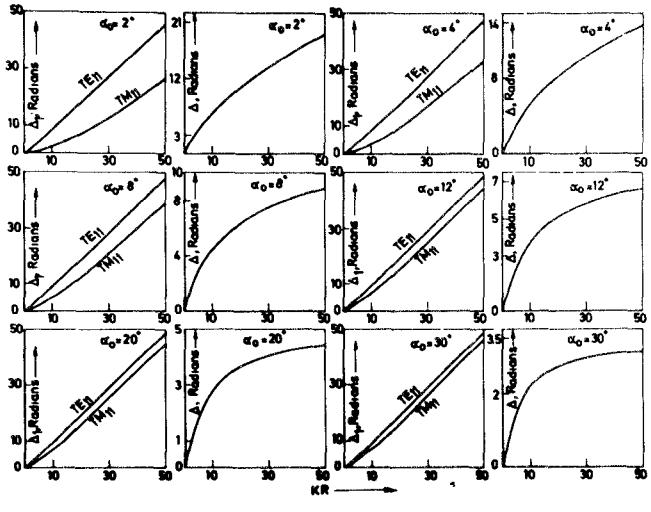

Fig. 6. Variation of phase shift for the TE_{11} and TM_{11} modes with α_0.

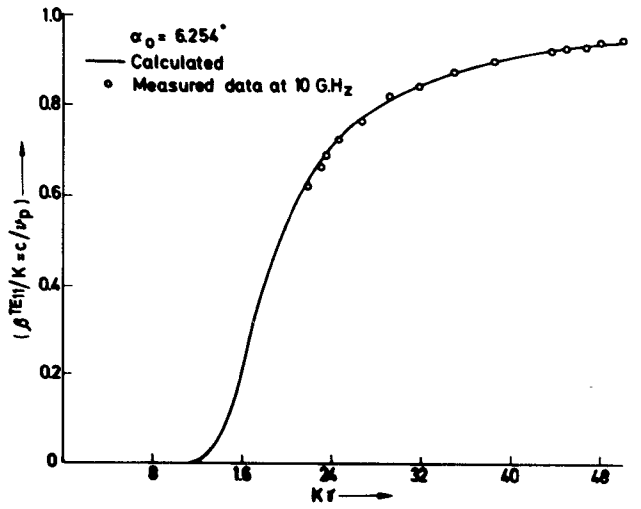

Fig. 7. Comparison of calculated and measured values for β/k for the TE_{11} mode.

has also been presented in the same figure for several values of α_0.[3] It has also been assumed here that the TE_{11} and TM_{11} modes are in phase at a radial distance $\alpha_1 = y$, where y is the eigenvalue for the TM_{11} mode for a prescribed α_0, since given a spherical mode, a cutoff radius may be approximately defined by $kr_c \doteq y$.

Finally, in order to examine the validity of the analytical procedure employed to study the transmission characteristics of spherical TE and TM modes in conical waveguides, measured data on (β/k) for a cone with $\alpha_0 = 6.254°$ at 10 GHz has been compared with the computed results in Fig. 7 for the TE_{11} mode. Excellent agreement between the two justifies the validity of the analysis presented.

IV. CONCLUSIONS

In conclusion one observes that a detailed study of the transmission characteristics of spherical TE and TM modes in conical waveguides is facilitated by accurate computation of eigenvalues. Further, the digital-computer based iterative procedure proposed for the evaluation of accurate eigenvalues of the spherical waves has been found to be very fast and highly accurate. Study of transmission characteristics of the spherical TE and TM modes within the guide has revealed a number of interesting properties. Explicit expressions are derived for various transmission parameters (attenuation constant, phase constant, and the wave impedance) associated with the mode transmission in a conical waveguide. These parameters are dependent on α_0 as well as the radial distance kr. A particular mode transmitted in a conical waveguide has to pass through an attenuation and a transmission region. The former is confined to the vicinity of the apex where the induction field predominates. At distances far away $(kr \geq y)$ from the apex there is a region of unattenuated transmission. A study of the phase slip between the spherical TE_{11} and TM_{11} modes transmitted simultaneously in a dual-mode conical waveguide has also been made. Experimental verification of the computed results on phase velocity of the spherical modes in conical waveguides justifies the validity of the analysis presented.

ACKNOWLEDGMENT

The authors wish to thank Dr. A. C. Ludwig, Jet Propulsion Laboratory, California Institute of Technology, California, for having supplied measured data on the phase velocity in a conical waveguide. They also wish to thank the Computer Center, IIT-Madras for having provided the facilities of IBM-370/155 System for the numerical computations involved in this short paper.

[3] It may be pointed out that the lower limit of the integral (2) is taken to be $\alpha_1 = y$ (where "y" is the eigenvalue for the TM_{11} mode) since one is primarily interested in the relative phase shift between the dominant spherical TE and TM modes in a dual mode conical waveguide. Further, in a dual-mode concial waveguide, the TM_{11} mode is generated by introducing a discontinuity at a radial distance $kr_1 = y$. Hence it follows that $\alpha_1 = kr_1 = y$.

REFERENCES

[1] E. C. Okress, *Microwave Power Engineering*, vol. 1. New York: Academic, 1968, pp. 228–240.
[2] P. D. Potter, "A new horn antenna with suppressed side lobes and equal beamwidth," *Microwave J.*, vol. 6 pp. 71–78, June 1963.
[3] R. F. Harrington, *Time-Harmonic Electromagnetic Fields*. New York: McGraw-Hill, 1961, ch. 6.
[4] M. S. Narasimhan and B. V. Rao, "Hybrid modes in corrugated conical horns," *Electron. Lett.*, vol. 6, pp. 32–34, Jan. 1970.
[5] M. A. Abramovitz and A. I. Stegun, *Hand Book of Mathematical Functions*. New York: Dover, 1965, ch. 9.
[6] W. Magnus and F. Oberhettinger, *Formulas and Theorems for the Functions of Mathematical Physics*. New York: Chelsea, 1954, pp. 72 and 67.
[7] J. M. McCormick and M. G. Salvadori, *Numerical Methods in Fortran*. Englewood Cliffs: N. J.: Prentice-Hall, 1964, ch. 4.

Simple Stabilizing Method for Solid-State Microwave Oscillators

A. KONDO, T. ISHII, AND K. SHIRAHATA

***Abstract*—In the microwave solid-state oscillators using bulk effect and avalanche diodes, high dielectric constant ceramics have been used as a temperature compensator and excellent temperature stability is obtained. An X-band avalanche diode oscillator is tested over a wide temperature range. The frequency drift is improved to be less than +30 kHz/°C. Additional advantages of this technique are compact size and low cost.**

I. INTRODUCTION

A simple means of reducing the noise and stabilizing the solid-state microwave oscillator is to use a high-Q cavity stabilizer. A phase lock technique has also been used by means of an injected signal and a mechanical compensation method which uses a tuning rod having a large temperature coefficient of expansion in the cavity. But these methods are fairly troublesome.

In this short paper, simple stabilizing methods using a ceramic dielectric are described. A ceramic dielectric which has a negative temperature coefficient is loaded in parallel with the diode package. The change of the diode and circuit reactance with temperature can be compensated by the capacitance change of the dielectric. A temperature coefficient less than +30 kHz/°C is obtained in a low-Q X-band cavity. These methods have merits of simplicity and low cost.

II. TEMPERATURE STABILIZATION WITH A DIELECTRIC

The effect of temperature on the diode reactance is due to the variation of the carrier velocity and the derivative of the ionization coefficient. These two parameters decrease with the temperature increase and it results in the increase of diode inductance. The increase of reactance causes the oscillation frequency to shift lower when the bias current is held constant. The cavity expansion due to the temperature rise also invites the same results on frequency characteristics.

If the change of diode and cavity reactance is trimmed with a ceramic capacitor having negative temperature coefficient, the oscillator would maintain the same frequency over the operating temperature range. Some titanium oxide dielectrics have negative temperature coefficients of capacitance [1]. Fortunately, its dielectric losses are the same order of alumina ceramics which are used for the microwave diode's package. In the following, we consider the circuit parameters to be represented by lumped constants. Judging from experimental results this assumption is reasonable at X band.

The oscillation frequency of an avalanche diode oscillator decreases almost rectilinearly with the temperature rise. We consider such an equivalent circuit as Fig. 1. C_p is the capacitance of the diode package and it changes very little with temperature. L_e is the equivalent inductance of the oscillator circuit. G and G_e represent

Manuscript received May 28, 1974.
The authors are with the Central Research Laboratory, Mitsubishi Electric Corporation, Itami, Hyogo, Japan.